

**FIFTEENTH INTERNATIONAL CONFERENCE ON PLASMA PHYSICS
AND CONTROLLED NUCLEAR FUSION RESEARCH**

Seville, Spain, 26 September - 1 October 1994

IAEA-CN-60/A-2-IV-3

High Beta Experiments in CHS

S. Okamura, K. Matsuoka, K. Nishimura, K. Tsumori,
R. Akiyama, S. Sakakibara, H. Yamada, S. Morita, T. Morisaki,
N. Nakajima, K. Tanaka, J. Xu, K. Ida, H. Iguchi, A. Lazaros,
T. Ozaki, H. Arimoto, A. Ejiri, M. Fujiwara, H. Idei, A. Iiyoshi,
O. Kaneko, K. Kawahata, T. Kawamoto, S. Kubo, T. Kuroda,
O. Motojima, V.D. Pustovitov, A. Sagara, C. Takahashi,
K. Toi and I. Yamada

(Received - Aug. 26, 1994)

NIFS-303

Sep. 1994

This report was prepared as a preprint of work performed as a collaboration research of the National Institute for Fusion Science (NIFS) of Japan. This document is intended for information only and for future publication in a journal after some rearrangements of its contents.

Inquiries about copyright and reproduction should be addressed to the Research Information Center, National Institute for Fusion Science, Nagoya 464-01, Japan.

HIGH BETA EXPERIMENTS IN CHS

S. Okamura, K. Matsuoka, K. Nishimura, K. Tsumori, R. Akiyama, S. Sakakibara,
H. Yamada, S. Morita, T. Morisaki, N. Nakajima, K. Tanaka, J. Xu, K. Ida,
H. Iguchi, A. Lazaros¹, T. Ozaki, H. Arimoto², A. Ejiri, M. Fujiwara, H. Idei,
A. Iiyoshi, O. Kaneko, K. Kawahata, T. Kawamoto, S. Kubo, T. Kuroda,
O. Motojima, V. D. Pustovitov³, A. Sagara, C. Takahashi, K. Toi and I. Yamada

National Institute for Fusion Science, Nagoya 464-01, Japan

1) *European Community Science and Technology Program*

2) *Plasma Science Center, Nagoya University, Nagoya 464-01, Japan*

3) *Permanent address : Kurchatov Institute, Moscow, Russia*

ABSTRACT

HIGH BETA EXPERIMENTS IN CHS

High beta experiments were performed in the low-aspect-ratio helical device CHS with the volume-averaged equilibrium beta up to 2.1 %. These values (highest for helical systems) are obtained for high density plasmas in low magnetic field heated with two tangential neutral beams. Confinement improvement given by means of turning off gas puffing helped significantly to make high betas. Magnetic fluctuations increased with increasing beta, but finally stopped to increase in the beta range $\langle \beta \rangle > 1$ %. The coherent modes appearing in the magnetic hill region showed strong dependence on the beta values. The dynamic poloidal field control was applied to suppress the outward plasma movement with the plasma pressure. Such an operation gave fixed boundary operations of high beta plasmas in helical systems.

Keywords : CHS, high beta plasma, self-stabilization, magnetic well, Mercier criterion, magnetic fluctuation, position control

1. INTRODUCTION

CHS is a heliotron/torsatron device (toroidal/poloidal mode numbers are $m=8/\ell=2$, major/minor radii are $R=1$ m/ $a=0.2$ m) which has a low aspect ratio ($A_p = 5$) among varieties of helical system designs [1]. The vacuum rotational transform increases from the center $\iota(0) \sim 0.3$ to the edge $\iota(a) \sim 1.0$. Magnetic shear is stronger at the edge. In high beta configurations, a large Shafranov shift forms a magnetic well in the central region which also increases the magnetic shear at the boundary as well. Figure 1 shows the Mercier stability conditions for the magnetic configuration which was used in the high beta experiments. The pressure profile is assumed to be proportional to $p_{eq}(r) = 1.71 (1 - (r/a)^{1.7})^{1.5} \times 10^{16}$ eV/cm³ which was obtained from the complete plasma profile measurements (n_e , T_e , T_i) for the $\langle \beta \rangle = 0.7\%$ discharge. The self-stabilization effect is expected to come out for high beta plasmas [2].

The magnetic well structure in CHS depends on the plasma position. An outward shifted configuration has a magnetic well in its vacuum field. The magnetic fluctuation signal decreases when the plasma position is shifted outward with the vertical field control. However the global confinement database of NBI discharges shows better confinement for the inward shifted case [3]. Since the limitation of beta is given by the confinement in the present status of CHS experiments, the inward shifted configuration was used for high beta experiments.

2. HIGH BETA DISCHARGES

Figure 2 shows the time behavior of one of highest beta discharges. Two NBIs (hydrogen beam) were used in balanced tangential injection (1.8 MW port-through power). Strong gas puff (hydrogen) was turned off when the plasma energy started to decrease because of the confinement degradation at the high density limit. The diamagnetic beta value increased during the decreasing phase of the density (reheat mode [4]) and got to the peak value 2.0% with the average density $n_e = 6.5 \times 10^{19}$ m⁻³ and the average magnetic field 0.57 T. The equilibrium calculation including beam contribution gives 2.1% average

equilibrium beta which is the highest beta value so far realized in helical systems.

Titanium gettering was used for the wall conditioning. The repetitive use of Ti gettering increased the practical density limit gradually which gave an increase in beta. The beta values are plotted as a function of the average density in Fig. 3. For the data points with gas puffing (open circles), betas are almost proportional to the densities. The beta values larger than 1.7 % are obtained with the reheat mode which appears only for the densities $n_e > 5.5 \times 10^{13} \text{ cm}^{-3}$. Because high beta discharges are made with limits of operational parameters (low magnetic field and high density), the global energy confinement time is lower than the LHD confinement scaling [5] ($\tau_E/\tau_{E,LHD} \sim 0.6$ during gas puffing). The reheat mode operation gave 30 % improvement of confinement to those high density operations. It was reported [6] that for the discharges with the average beta $\langle\beta\rangle < 1.5$ %, no degradation of global confinement had been observed in comparison with the LHD scaling. The conclusion is extended now for $\langle\beta\rangle \leq 2.1$ %.

3. MAGNETIC FLUCTUATION MEASUREMENTS

Figure 4(a) shows the dependence of magnetic fluctuations (3-100 kHz) on the average betas. The root mean square values at the probe position normalized by the equilibrium poloidal field are plotted. Closed circles in a low beta region $\langle\beta\rangle < 0.5$ % give maximum values of continual burst type coherent signals ($m/n=2/1$, m :poloidal mode number/ n :toroidal) which appear only with a single beam injection in the co-direction. Continuous signal levels increased almost in proportion to the beta value for $\langle\beta\rangle < 1$ %, but it stopped to increase for $\langle\beta\rangle > 1$ %. Coherent components with $m \leq 2$ are replotted in Fig. 4(b). Each mode appeared in a different region of beta values. The $m/n=2/1$ mode increased rapidly with beta value up to 1 %, while it decreased for higher beta values and finally disappeared for $\langle\beta\rangle > 1.4$ %. The $n/n=1/1$ mode appeared for $\langle\beta\rangle > 0.5$ % together with $m/n=3/2$ and $4/3$ modes which are in small amplitudes. The $m/n=1/1$ (or $2/2$) mode became largest coherent mode for $\langle\beta\rangle > 1.3$ %.

Stationary fluctuations with $m/n < 2$ except the burst type fluctuations are possibly resistive interchange modes because they appeared in the magnetic hill region which is Mercier stable. The experimental observations tell that the saturation level of those fluctuations did not increase for $\langle \beta \rangle > 1\%$. Comparison with theoretical model is needed to understand those dependence.

4. DYNAMIC POLOIDAL FIELD CONTROL

The plasma position moves outward by 0.8 cm when the plasma beta reaches 2%. The formation of self-induced magnetic well is the combined effect of such an outward shift of magnetic surfaces and the Shafranov shift. The dynamic poloidal field control (PFC) during the discharge was made in order to fix the plasma boundary position when the plasma beta increased. This method is useful also in a technical sense when it is requested to fix the plasma boundary during a high beta discharge, from the aspect of interference between the plasma boundary and the plasma periphery conditions such as the limiters or divertors. Figure 5(a) shows the outward movement of plasma edge density profile measured with a lithium beam probe in no PFC discharge. When the poloidal field was varied as shown in Fig. 5(b), such a movement was suppressed as shown in Fig. 5(c). When the shift of plasma column is suppressed, the self-stabilization effect of magnetic well becomes smaller. Nevertheless the average beta increased by about 10% with PFC which is due to the effect of global confinement dependence on the plasma position in CHS. The magnetic fluctuations in PFC discharges were roughly 1.5 times larger compared with no PFC discharges which also reflects the general dependence of magnetic fluctuations in CHS on the plasma position.

REFERENCES

- [1] NISHIMURA, K., et al., *Fusion Technol.* **17** (1990) 86.
- [2] ICHIGUCHI, K., et al., *Nucl. Fusion* **33** (1993) 481.
- [3] HARRIS, J.H., et al., *Phys. Rev. Lett.* **63** (1989) 1249.
- [4] KANEKO, O., et al., in *Plasma Physics and Controlled Fusion Research 1990* (Proc. 13th Int. Conf. Washington, 1990), Vol. 2, IAEA, Vienna (1991) 474.
- [5] MORITA, S., et al., in *Plasma Physics and Controlled Fusion Research 1992* (Proc. 14th Int. Conf. Würzburg, 1992), Vol. 2, IAEA, Vienna (1993) 515.
- [6] SUDO, S., et al., *Nucl. Fusion* **30** (1990) 11.
- [7] YAMADA, H., et al., in *Plasma Physics and Controlled Fusion Research 1992* (Proc. 14th Int. Conf., Würzburg 1992) Vol. 2, IAEA, Vienna (1993) 493.

Figure Captions

- Fig. 1 Contour map of normalized Mercier stability criterion D_1 for CHS. The D_1 is defined as $D_1 \equiv -D_M/\tau'^2$, where D_M is the standard Mercier criterion [2]. The region surrounded by a thick solid line is Mercier unstable : $D_1 \geq 0$. Thinner lines give contours with steps $\Delta D_1 = 0.2$.
- Fig. 2 Time behavior of high beta discharge. (a) diamagnetic average beta, (b) line-averaged density, (c) gas puffing rate (hydrogen), (d) NBI absorbed power (P_{in}) and radiation power (P_{rad}).
- Fig. 3 Diamagnetic average beta as a function of line-averaged density. Open circles are for maximum beta values during gas puffing, while double circles are for peak beta values in reheat mode.
- Fig. 4 Magnetic fluctuations plotted as a function of diamagnetic average betas. (a) root mean square(rms) values of total fluctuation level at probe position normalized by the equilibrium poloidal field : $B_p \equiv \alpha \tau(\alpha) B_t / R$. For burst type signals, the maximum rms values are plotted. (b) rms values of coherent components which have poloidal mode number $m \leq 2$.
- Fig. 5 Time evolutions of edge density profiles measured with lithium beam probe for (a) no poloidal field control and (c) dynamic poloidal field control. The horizontal axis is the distance along the lithium beam injection at the toroidal position where the magnetic surfaces are horizontally elongated. (b) shows relative timing of dynamic poloidal field control to the plasma discharge. Currents in three poloidal coils are varied to make 2 cm inward shift of magnetic axis in vacuum configurations.

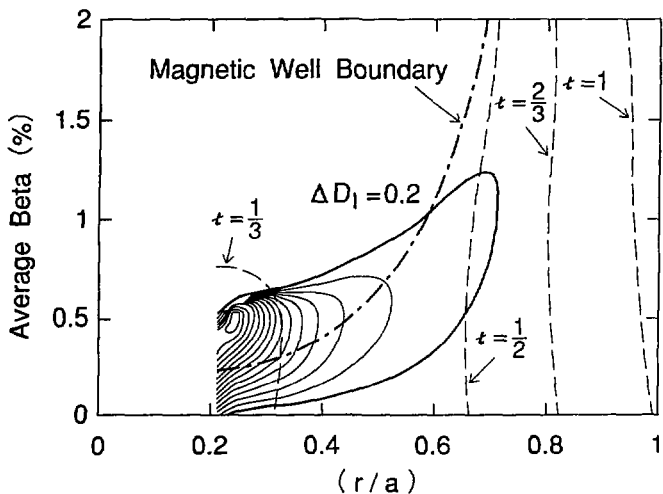


Fig. 1 Contour map of normalized Mercier stability criterion D_1 for CHS. The D_1 is defined as $D_1 = -D_M/\tau^2$, where D_M is the standard Mercier criterion [2]. The region surrounded by a thick solid line is Mercier unstable: $D_1 \geq 0$. Thinner lines give contours with steps $\Delta D_1 = 0.2$.

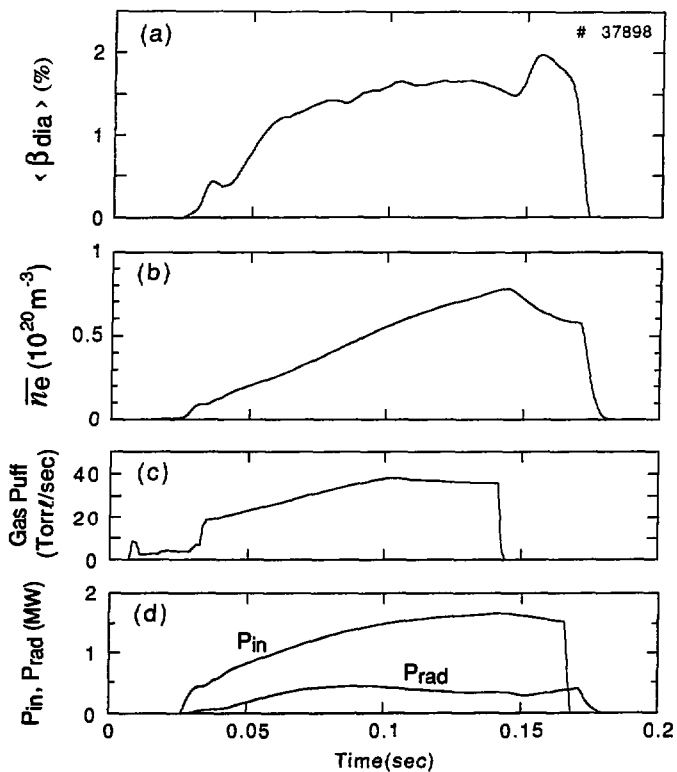


Fig. 2 Time behavior of high beta discharge. (a) diamagnetic average beta, (b) line-averaged density, (c) gas puffing rate (hydrogen), (d) NBI absorbed power (P_{in}) and radiation power (P_{rad}).

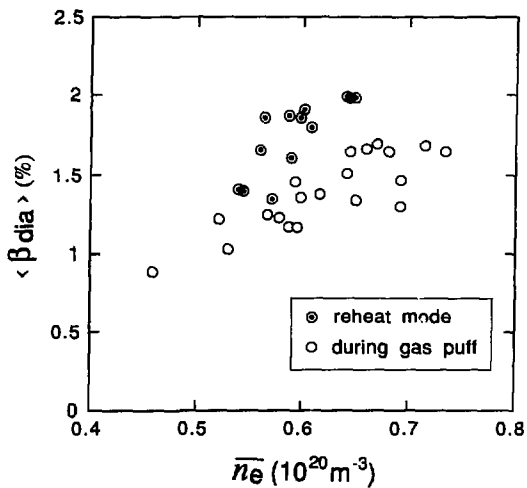


Fig. 3 Diamagnetic average beta as a function of line-averaged density. Open circles are for maximum beta values during gas puffing, while double circles are for peak beta values in reheat mode.

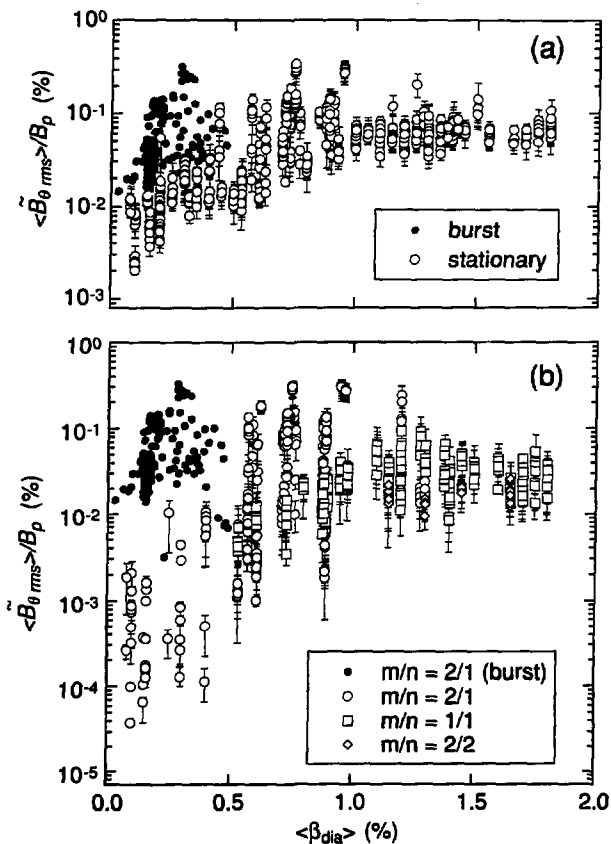


Fig. 4 Magnetic fluctuations plotted as a function of diamagnetic average betas. (a) root mean square(rms) values of total fluctuation level at probe position normalized by the equilibrium poloidal field: $B_p = a \tau(\alpha) B_T / R$. For burst type signals, the maximum rms values are plotted. (b) rms values of coherent components which have poloidal mode number $m \leq 2$.

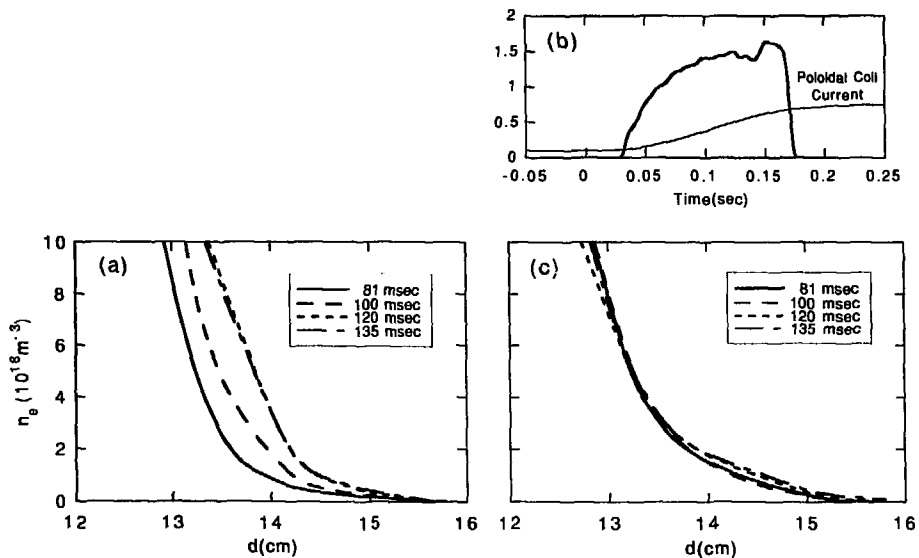


Fig. 5 Time evolutions of edge density profiles measured with lithium beam probe for (a) no poloidal field control and (c) dynamic poloidal field control. The horizontal axis is the distance along the lithium beam injection at the toroidal position where the magnetic surfaces are horizontally elongated. (b) shows relative timing of dynamic poloidal field control to the plasma discharge. Currents in three poloidal coils are varied to make 2 cm inward shift of magnetic axis in vacuum configurations.

Recent Issues of NIFS Series

- NIFS-262 V.D.Pustovitov,
Some Theoretical Problems of Magnetic Diagnostics in Tokamaks and Stellarators; Dec. 1993
- NIFS-263 A. Fujisawa, H. Iguchi, Y. Hamada
A Study of Non-Ideal Focus Properties of 30° Parallel Plate Energy Analyzers; Dec. 1993
- NIFS-264 K. Masai,
Nonequilibrium in Thermal Emission from Supernova Remnants;
Dec. 1993
- NIFS-265 K. Masai, K. Nomoto,
X-Ray Enhancement of SN 1987A Due to Interaction with its Ring-like Nebula; Dec. 1993
- NIFS-266 J. Uramoto
A Research of Possibility for Negative Muon Production by a Low Energy Electron Beam Accompanying Ion Beam; Dec. 1993
- NIFS-267 H. Iguchi, K. Ida, H. Yamada, K. Itoh, S.-I. Itoh, K. Matsuoka,
S. Okamura, H. Saruki, I. Yamada, H. Takenaga, K. Uchino, K. Muraoka,
The Effect of Magnetic Field Configuration on Particle Pinch Velocity in Compact Helical System (CHS); Jan. 1994
- NIFS-268 T. Shikama, C. Namba, M. Kosuda, Y. Maeda,
Development of High Time-Resolution Laser Flash Equipment for Thermal Diffusivity Measurements Using Miniature-Size Specimens;
Jan. 1994
- NIFS-269 T. Hayashi, T. Sato, P. Merkel, J. Nührenberg, U. Schwenn,
Formation and 'Self-Healing' of Magnetic Islands in Finite- β Helias Equilibria; Jan. 1994
- NIFS-270 S. Murakami, M. Okamoto, N. Nakajima, T. Mutoh,
Efficiencies of the ICRF Minority Heating in the CHS and LHD Plasmas; Jan. 1994
- NIFS-271 Y. Nejob, H. Saruki,
Large Amplitude Langmuir and Ion-Acoustic Waves in a Relativistic Two-Fluid Plasma; Feb. 1994
- NIFS-272 A. Fujisawa, H. Iguchi, A. Taniike, M. Sasao, Y. Hamada,
A 6MeV Heavy Ion Beam Probe for the Large Helical Device;
Feb. 1994

- NIFS-273 Y. Hamada, A. Nishizawa, Y. Kawasumi, K. Narihara, K. Sato, T. Seki, K. Toi, H. Iguchi, A. Fujisawa, K. Adachi, A. Ejiri, S. Hidekuma, S. Hirokura, K. Ida, J. Koong, K. Kawahata, M. Kojima, R. Kumazawa, H. Kuramoto, R. Liang, H. Sakakita, M. Sasao, K. N. Sato, T. Tsuzuki, J. Xu, I. Yamada, T. Watari, I. Negi,
Measurement of Profiles of the Space Potential in JIPP T-IIU Tokamak Plasmas by Slow Poloidal and Fast Toroidal Sweeps of a Heavy Ion Beam; Feb. 1994
- NIFS-274 M. Tanaka,
A Mechanism of Collisionless Magnetic Reconnection; Mar. 1994
- NIFS-275 A. Fukuyama, K. Itoh, S.-I. Itoh, M. Yagi and M. Azumi,
Isotope Effect on Confinement in DT Plasmas; Mar. 1994
- NIFS-276 R.V. Reddy, K. Watanabe, T. Sato and T.H. Watanabe,
Impulsive Alfvén Coupling between the Magnetosphere and Ionosphere; Apr. 1994
- NIFS-277 J. Uramoto,
A Possibility of π^- Meson Production by a Low Energy Electron Bunch and Positive Ion Bunch; Apr. 1994
- NIFS-278 K. Itoh, S.-I. Itoh, A. Fukuyama, M. Yagi and M. Azumi,
Self-sustained Turbulence and L-mode Confinement in Toroidal Plasmas II; Apr. 1994
- NIFS-279 K. Yamazaki and K.Y. Watanabe,
New Modular Heliotron System Compatible with Closed Helical Divertor and Good Plasma Confinement; Apr. 1994
- NIFS-280 S. Okamura, K. Matsuoka, K. Nishimura, K. Tsumori, R. Akiyama, S. Sakakibara, H. Yamada, S. Morita, T. Morisaki, N. Nakajima, K. Tanaka, J. Xu, K. Ida, H. Iguchi, A. Lazaros, T. Ozaki, H. Arimoto, A. Ejiri, M. Fujiwara, H. Idei, O. Kaneko, K. Kawahata, T. Kawamoto, A. Komori, S. Kubo, O. Motojima, V.D. Pustovitov, C. Takahashi, K. Toi and I. Yamada,
High-Beta Discharges with Neutral Beam Injection in CHS; Apr. 1994
- NIFS-281 K. Kamada, H. Kinoshita and H. Takahashi,
Anomalous Heat Evolution of Deuteron Implanted Al on Electron Bombardment ; May 1994
- NIFS-282 H. Takamaru, T. Sato, K. Watanabe and R. Horiuchi,
Super Ion Acoustic Double Layer; May 1994
- NIFS-283 O. Mitarai and S. Sudo
Ignition Characteristics in D-T Helical Reactors; June 1994

- NIFS-284 R. Horiuchi and T. Sato,
Particle Simulation Study of Driven Magnetic Reconnection in a Collisionless Plasma; June 1994
- NIFS-285 K.Y. Watanabe, N. Nakajima, M. Okamoto, K. Yamazaki, Y. Nakamura, M. Wakatani,
Effect of Collisionality and Radial Electric Field on Bootstrap Current in LHD (Large Helical Device); June 1994
- NIFS-286 H. Sanuki, K. Itoh, J. Todoroki, K. Ida, H. Idei, H. Iguchi and H. Yamada,
Theoretical and Experimental Studies on Electric Field and Confinement in Helical Systems; June 1994
- NIFS-287 K. Itoh and S.-I. Itoh,
Influence of the Wall Material on the H-mode Performance; June 1994
- NIFS-288 K. Itoh, A. Fukuyama, S.-I. Itoh, M. Yagi and M. Azumi
Self-Sustained Magnetic Braiding in Toroidal Plasmas; July 1994
- NIFS-289 Y. Nejh,
Relativistic Effects on Large Amplitude Nonlinear Langmuir Waves in a Two-Fluid Plasma; July 1994
- NIFS-290 N. Ohyabu, A. Komori, K. Akaishi, N. Inoue, Y. Kubota, A.I. Livshit, N. Noda, A. Sagara, H. Suzuki, T. Watanabe, O. Motojima, M. Fujiwara, A. Iiyoshi,
Innovative Divertor Concepts for LHD; July 1994
- NIFS-291 H. Idei, K. Ida, H. Sanuki, S. Kubo, H. Yamada, H. Iguchi, S. Morita, S. Okamura, R. Akiyama, H. Arimoto, K. Matsuoka, K. Nishimura, K. Ohkubo, C. Takahashi, Y. Takita, K. Toi, K. Tsumori and I. Yamada,
Formation of Positive Radial Electric Field by Electron Cyclotron Heating in Compact Helical System; July 1994
- NIFS-292 N. Noda, A. Sagara, H. Yamada, Y. Kubota, N. Inoue, K. Akaishi, O. Motojima, K. Iwamoto, M. Hashiba, I. Fujita, T. Hino, T. Yamashina, K. Okazaki, J. Rice, M. Yamage, H. Toyoda and H. Sugai,
Boronization Study for Application to Large Helical Device; July 1994
- NIFS-293 Y. Ueda, T. Tanabe, V. Philipps, L. Könen, A. Pospieszczyk, U. Samm, B. Schweer, B. Unterberg, M. Wada, N. Hawkes and N. Noda,
Effects of Impurities Released from High Z Test Limiter on Plasma Performance in TEXTOR; July. 1994
- NIFS-294 K. Akaishi, Y. Kubota, K. Ezaki and O. Motojima,
Experimental Study on Scaling Law of Outgassing Rate with A Pumping Parameter, Aug. 1994

- NIFS-295 S. Bazdenkov, T. Sato, R. Horiuchi, K. Watanabe
Magnetic Mirror Effect as a Trigger of Collisionless Magnetic Reconnection, Aug. 1994
- NIFS-296 K. Itoh, M. Yagi, S.-I. Itoh, A. Fukuyama, H. Sanuki, M. Azumi
Anomalous Transport Theory for Toroidal Helical Plasmas, Aug. 1994 (IAEA-CN-60/D-III-3)
- NIFS-297 J. Yamamoto, O. Motojima, T. Mito, K. Takahata, N. Yanagi, S. Yamada, H. Chikaraishi, S. Imagawa, A. Iwamoto, H. Kaneko, A. Nishimura, S. Satoh, T. Satow, H. Tamura, S. Yamaguchi, K. Yamazaki, M. Fujiwara, A. Iiyoshi and LHD group,
New Evaluation Method of Superconductor Characteristics for Realizing the Large Helical Device; Aug. 1994 (IAEA-CN-60/F-P-3)
- NIFS-298 A. Komori, N. Ohyabu, T. Watanabe, H. Suzuki, A. Sagara, N. Noda, K. Akaishi, N. Inoue, Y. Kubota, O. Motojima, M. Fujiwara and A. Iiyoshi,
Local Island Divertor Concept for LHD; Aug. 1994 (IAEA-CN-60/F-P-4)
- NIFS-299 K. Toi, T. Morisaki, S. Sakakibara, A. Ejiri, H. Yamada, S. Morita, K. Tanaka, N. Nakjima, S. Okamura, H. Iguchi, K. Ida, K. Tsumori, S. Ohdachi, K. Nishimura, K. Matsuoka, J. Xu, I. Yamada, T. Minami, K. Narihara, R. Akiyama, A. Ando, H. Arimoto, A. Fujisawa, M. Fujiwara, H. Idei, O. Kaneko, K. Kawahata, A. Komori, S. Kubo, R. Kumazawa, T. Ozaki, A. Sagara, C. Takahashi, Y. Takita and T. Watari
Impact of Rotational-Transform Profile Control on Plasma Confinement and Stability in CHS; Aug. 1994 (IAEA-CN-60/A6/C-P-3)
- NIFS-300 H. Sugama and W. Horton,
Dynamical Model of Pressure-Gradient-Driven Turbulence and Shear Flow Generation in L-H Transition; Aug. 1994 (IAEA/CN-60/D-P-I-11)
- NIFS-301 Y. Hamada, A. Nishizawa, Y. Kawasumi, K.N. Sato, H. Sakakita, R. Liang, K. Kawahata, A. Ejiri, K. Narihara, K. Sato, T. Seki, K. Toi, K. Itoh, H. Iguchi, A. Fujisawa, K. Adachi, S. Hidekuma, S. Hirokura, K. Ida, M. Kojima, J. Koog, R. Kumazawa, H. Kuramoto, T. Minami, I. Negi, S. Ohdachi, M. Sasao, T. Tsuzuki, J. Xu, I. Yamada, T. Watari,
Study of Turbulence and Plasma Potential in JIPP T-IIU Tokamak; Aug. 1994 (IAEA/CN-60/A-2-III-5)
- NIFS-302 K. Nishimura, R. Kumazawa, T. Mutoh, T. Watari, T. Seki, A. Ando, S. Masuda, F. Shinpo, S. Murakami, S. Okamura, H. Yamada, K. Matsuoka, S. Morita, T. Ozaki, K. Ida, H. Iguchi, I. Yamada, A. Ejiri, H. Idei, S. Muto, K. Tanaka, J. Xu, R. Akiyama, H. Arimoto, M. Isobe, M. Iwase, O. Kaneko, S. Kubo, T. Kawamoto, A. Lazaros, T. Morisaki, S. Sakakibara, Y. Takita, C. Takahashi and K. Tsumori,
ICRF Heating in CHS; Sep. 1994 (IAEA-CN-60/A-6-I-4)